Proceedings of the Korean Nuclear Society Spring Meeting
Cheju, Korea, May 2001

Assessment of RELAP5/MOD3.2.2beta Code for the LOFT L9-1 Experiment

Kyu Bok Lee, Hee Do Lee, Kye Kwang Jee
Korea Power Engineering Company, Inc.
360-9 Mabuk-ri, Guseong-eup, Yongin-si, Gyeonggi-do, Korea 449-713
Young Seok Bang
Korea Institute of Nuclear Safety, Yusung, Taejon, Korea 305-600
Chang Hyo Kim
Seoul National University, San 56-1, Sillim-dong, Kwanak-gu, Seoul, Korea 151-742

Abstract

The RELAP5/MOD3.2.2beta code was assessed on the predictability of the thermal-hydraulic phenomena in primary and secondary coolant system during the LOFT test L9-1. The L9-1 test performed at the LOFT facility was an experiment to simulate a total loss of feedwater (TLOFW) accident with delayed reactor scram and no auxiliary feedwater injection. From comparisons of the code predicted results with experimental data, it was concluded that the code was capable of simulating the thermal-hydraulic behavior during the short term phase of LOFT L9-1 test. In addition, it was identified that three parameters such as the steam generator (SG) nodalization, SG U-tube heat transfer area, and loss coefficient of the pressurizer spray valve had a significant effect on the calculation results for the LOFT test L9-1.

1. Introduction

The total loss of feedwater (TLOFW) accident is a beyond-design-basis-accident initiated by a loss of feedwater due to failure of the main feedwater pump and no auxiliary feedwater injection. During the TLOFW, heat removal capacity in the SG secondary side is degraded and primary coolant system (PCS) pressure and temperature are increased, which results in a reactor scram. The increasing PCS pressure due to decay heat following the reactor scram is controlled by over-pressure protection systems such as a pressurizer spray valve and power operated relief valve (PORV).

The objective of this analysis is to assess the capability of the RELAP5/MOD3.2.2beta computer code to predict thermal-hydraulic behavior during the TLOFW. The analysis was performed based on the previous calculation for the LOFT test L9-1. The input data for this analysis was prepared by modifying some parameters which were identified from sensitivity studies having a significant effects on the predicted thermal-hydraulic behaviors. To assess the predictability of the code, the calculation results are compared with the L9-1 experiment performed at the LOFT facility to simulate the TLOFW accident.

2. Experimental Facility and Test

The LOFT integral test facility[1] is a scale model of a PWR. The intent of the facility is to model the nuclear, thermal-hydraulic phenomena which can take place in a PWR during a loss of coolant accident (LOCA). It is a scaled representation of a commercial PWR of Westinghouse type having 4 loops with a volume ratio of 1/60. The general philosophy in scaling coolant volumes and flow areas in the LOFT was to use the ratio of LOFT core(50 MWt) to PWR core (3000MWt). The LOFT facility is designed to simulate the major components and system responses of a commercial PWR. The experimental assembly consists of five major subsystems which are instrumented such that system variables can be measured and recorded during an experiment. The subsystems include (a) the reactor vessel, (b) the intact loop, (c) the broken loop, (d) the blowdown suppression system, and (e) the emergency core cooling system(ECCS). The heights of the core and reactor vessel of the LOFT facility are 1.68 and 7 m, respectively.

Test L9-1 was part of the two sequential tests of L9-1/L3-3[2,3,4]. The L9-1 experiment simulated a LOFA with delayed scram and no auxiliary feedwater injection in PWR, while the subsequent test L3-3 described the LOFA recovery modes initiated by tripping the primary coolant pump (PCP) and depressurizing the PCS through the pressurizer power operated relief valve (PORV). Prior to the experiment, the flow rate of the primary system was 479.1±2.6 kg/sec under a pressure of 14.9±0.10 MPa. Temperatures of the hot leg and cold leg of the intact loop were 578.2±1.8 K and 558.9±1.3 K, respectively. The important initial conditions are listed in Table 1.

The major objective of test L9-1 was to evaluate uncertainties in predicted primary and secondary thermal hydraulic response associated with the steam generator dry-out during delayed scram. The L9-1 experiment was initiated by turning off the main feedwater pump. Due to the decrease in heat removal capacity of the SG secondary side, PCS pressure increased and the pressurizer spray valve was observed to open at its set point(15.338 MPa), 30.0 seconds after initiation of LOFA. As the magnitude of the primary-secondary power mismatch grew, the PCS pressurization exceeded the cooling capability of the pressurizer spray. The reactor scrammed on indication of high pressure (15.745 MPa) in the intact hot leg at approximately 65 seconds. The auxiliary feedwater injection into the SG was prevented, as was scram on indication of low liquid level in the SG. The main steam control valve (MSCV) began to close automatically on the reactor scram signal and was completely closed at 77.2 seconds. The primary system pressure dropped on the reactor scram, and began to rise again due to decay heat and the complete loss of heat sink in the SG secondary side, which resulted in pressurizer spray valve cycling at 208.9 seconds. The open/close set points of the pressurizer spray valve were 15.338 and 15.05 MPa, respectively. The pressurizer spray was allowed to cycle for approximately 900 seconds, whereupon it was closed by the operators, allowing PCS pressure to rise to the PORV actuation setpoint (16.20 MPa) at 1468 seconds. Thereafter, the pressurizer became liquid-full state. The PORV was allowed to cycle at 1467.9 seconds to relieve primary coolant as the PCS volume continued to heatup and expand. The PORV cycling was stopped at 3270 seconds, when the PCS hot leg temperature reached 597 K. At that time, the subsequent test of L3-3 was initiated.

3. Analysis Code and Modeling

RELAP5/MOD3.2.2beta version[5], in which several new models and improvements have been incorporated , is used in the present assessment calculation for the test L9-1. The analysis was performed base on the previous calculation[4] which assessed RELAP5/MOD3/5m5 version for the LOFT test L9-1/L3-3. The input deck of the previous calculation was modified for this assessment to make the RELAP5/MOD3.2.2beta version be executable and to improve the calculation results. Major changes are as follows:

(1) Initial conditions of some volumes were modified to make the RELAP5/MOD3.2.2beta code be executable.
(2) The junction connected to the accumulator in addition to the one in the accumulator was removed in this analysis, because it was not allowed in the code version of RELAP5/MOD3.2.2beta. Since the emergency core cooling system (ECCS) is not injected during the test L9-1/L3-3, the junction removal to the accumulator does not affect the calculation results.
(3) The bottom node of the SG secondary side and associated nodes of the SG U-tube in the previous calculation were subdivided into four as shown in Figure 1.
(4) The heat transfer area of the bottom node of the SG U-tube in the previous calculation increased by about 20%.
(5) The loss coefficient of the pressurizer spray valve was set to zero.

It was identified from sensitivity studies that the three parameters mentioned above such as the SG nodalization, SG U-tube heat transfer area, and loss coefficient of the pressurizer spray valve have a significant effect on the calculated thermal-hydraulic behaviors.

The nodalization to simulate the LOFT facility consists of 134 volumes connected by 143 junctions and 142 heat structures as shown in Figure 1. The intact loop was modeled with 31 hydrodynamic volumes. All piping metal structures exposed to atmosphere were simulated with the heat structure to simulate the associated heat loss. The broken loop was composed of a hot leg, a SG-pump simulator, a reflood assist bypass system (RABS), a cold leg and quick opening blowdown valves (QOBVs). The volume and junction modeling options were set to the default options. The active core, the downcomer and the filler gap were composed of three volumes, six, and seven vertically stacked volumes, respectively. The rod bundle interphase friction model option was applied for the active core volumes. The fuel rods were modeled using 3 heat structures representing the central fuel assembly and 3 heat structures representing the peripheral fuel assemblies of the LOFT core. The pressurizer system was modeled with a surgeline, a pressurizer vessel, a spray line from cold leg, a spray valve and a PORV. Two volumes for the surge line, nine volumes for the vessel and one volume for the spray line were used. The spray valve and the PORV were simulated with two trip valves. The associated trip logic was prepared according to the experimental specification.

The SG was modeled using 12 volumes in the PCS and 8 volumes in the SG riser. Heat is exchanged between the primary and secondary sides of the SG via the U-tube, which was modeled by 12 heat structures. The rod bundle interphacial friction option was used for the volumes in contact with the U-tubes heat structures.

The emergency core cooling system (ECCS) in the LOFT was also modeled. However, it is not used in the transient calculation. The containment was modeled using a time-dependent volume with constant pressure.

A steady state run was performed to obtain initial conditions of the whole system prior to running the transient. The initial conditions obtained from the steady state run were compared with the measured data in Table 1. The RELAP5 steady state run results generally agree well with the experimental initial conditions.

4. Results and Discussion

The calculation results from the RELAP5/MOD3.2.2beta computer code for the LOFA transient were compared with LOFT integral test L9-1 results. In this evaluation, only the short term transient phase up to 300 seconds is determined and compared with experimental data, even though the transient test L9-1 duration was about 3270 seconds. Major thermal-hydraulic phenomena except for the over-pressure protection through the PORV can be observed during only the short term phase. The initial and boundary conditions used in the calculation were obtained from the steady state run.

The PCS pressure and temperature comparisons are shown in Figures 2 and 3. As the heat removal capacity in the SG secondary side was degraded from initiation of the LOFA, the PCS pressure and temperature were increased. The PCS pressure triggered the automatic reactor scram when it reached the set pressure of 15.745 MPa. Following the scram, the power input to the PCS dropped significantly because the reactor was operated at the decay power level. After the reactor scram, the PCS pressure and temperature start to rise again due to the decay power. The increased PCS pressure results in the cycling operation of the pressurizer spray. The pressurizer spraying temporarily brought down the PCS pressure. Figures 2 and 3 indicate that the calculation results are very similar to the experimental data, even though minor discrepancies of the PCS pressure are also identified. The code predicted reactor scram is slightly delayed, and the calculated PCS pressure just after reactor scram is lower than that of the experiment by about 0.5 MPa. However, these differences were not significant enough to affect the calculation results for the later analysis.

Figure 4 shows a comparison of the calculated reactor power to the experimental data. It is apparent that that the predicted behavior of the reactor power is in a good agreement with the experimental data.

A comparison of the SG secondary pressure and temperature from calculation and experiment is provided in Figures 5 and 6, respectively. The SCS pressure and temperature immediately following the transient rose gradually due to heating from the primary side. As the secondary side of SG was drying out, however, the reduced heat removal rate brought down the SCS pressure and temperature. The SG pressure and temperature increased again as the main steam control valve (MSCV) started to close on the scram signal. After the MSCV was closed, pressurization of both the PCS and SCS due to decay heat was controlled by pressurizer spray and subsequent steam condensation. As shown in Figures 5 and 6, the calculated thermal-hydraulic behaviors of the SG secondary side closely resemble the experiment.

Figure 7 shows a comparison of the SG collapsed liquid level. The SG secondary collapsed water level is a good indication of SG secondary conditions changing. According to Figure 7, the water level of the SG secondary side dropped monotonically due to evaporation without feed. As the water level decreased, the heat transfer rate through the SG U-tube decreased. The complete voiding of the SG secondary side was predicted to be 90 seconds by the code. This matches well with the L9-1 test data, even though the actual dry-out was occurred slightly earlier than for the code calculated prediction. Generally, it is apparent that the code calculated water level closely resembles the test data.

A comparison of the experimental and calculated mass flow rate through the MSCV is shown in Figure 8. From these comparisons, it can be stated that the mass flow behavior through the MSCV can be well predicted except for the slight difference in reactor scram times.

5. Conclusions

The RELAP5/MOD3.2.2beta code was assessed for the LOFT test L9-1 simulating TLOFW event. The calculation results were compared with the experimental data and the predictability for major thermal-hydraulic phenomena was also evaluated during a short term transient phase, with the following conclusions:

(1) RELAP5/MOD3.2.2beta code calculation successfully simulated the LOFT test L9-1 and the capability to model the TLOFW event was demonstrated.

(2) The RELAP5/MOD3.2.2beta code successfully predicted the general trend in primary and secondary coolant systems which demonstrates agreement with the experimental data.

(3) It was identified from sensitivity studies that three parameters such as the SG nodalization, SG U-tube heat transfer area, and loss coefficient of the pressurizer spray valve have a significant effect on the calculated thermal-hydraulic behaviors for the LOFT test L9-1.

(4) Several minor discrepancies were also identified. The code predicted timing of the reactor scram was slightly delayed, and the calculated pressure of the primary coolant system just after reactor scram was lower than that for the experiment. However, these differences were insignificant and did not adversely affect the calculation results for the later analysis.

References

1. D. L. Reeder, *LOFT system and Test Description*, NUREG/CR-0247, July 1978.
2. M. McCormick-Barger, *Experiment Data Report for LOFT Anticipated with Multiple Failures Experiment L9-1 and Small Break Experiment L3-3*, NUREG/CR-2119, June 1981.
3. J. Adams, *Quick-Look-Report on LOFT Nuclear Experiment L9-1/L3-3*, EGG-LOFT-5340, April 1981.
4. Y.S. Bang, et al, *Assessment of RELAP5/MOD3 with the LOFT L9-1/L3-3 Experiment Simulating an Anticipated Transient with Multiple Failures*, NUREG/IA-0114, February 1994.

5. Scientech, Inc., *RELAP5/MOD3 Code Manual*, Volume 1-7, March 1998.

Table 1 Initial conditions of the test L9-1

Parameter	Measured	Simulated
Primary Coolant System		
Mass flow rate (kg/s)	479.1±2.6	479.3
Hot leg pressure (MPa)	14.9±0.10	14.92
Cold leg temperature (K)	558.9±1.3	558.2
Hot leg temperature (K)	578.2±1.8	577.4
Reactor		
Power level (MW)	49.6±0.9	49.6
Steam Generator Secondary Side		
Water level (m)	0.14±0.08	0.14
Water temperature (k)	545.0±0.8	544.6
Pressure (MPa)	5.67±0.08	5.57
Mass flow rate (kg/s)	27.0±1.0	26.1
Broken Loop		
Hot leg temperature (K)	563.3±2.6	557.7
Cold leg temperature (K)	557.6±2.6	558.1
Pressurizer		
Steam Volume (m^3)	0.43±0.05	-
Liquid volume (m^3)	0.50±0.05	-
Water temperature (K)	614.9±1.3	613.6
Pressure (MPa)	14.93±0.25	14.93
Liquid level (m)	0.92±0.1	0.94

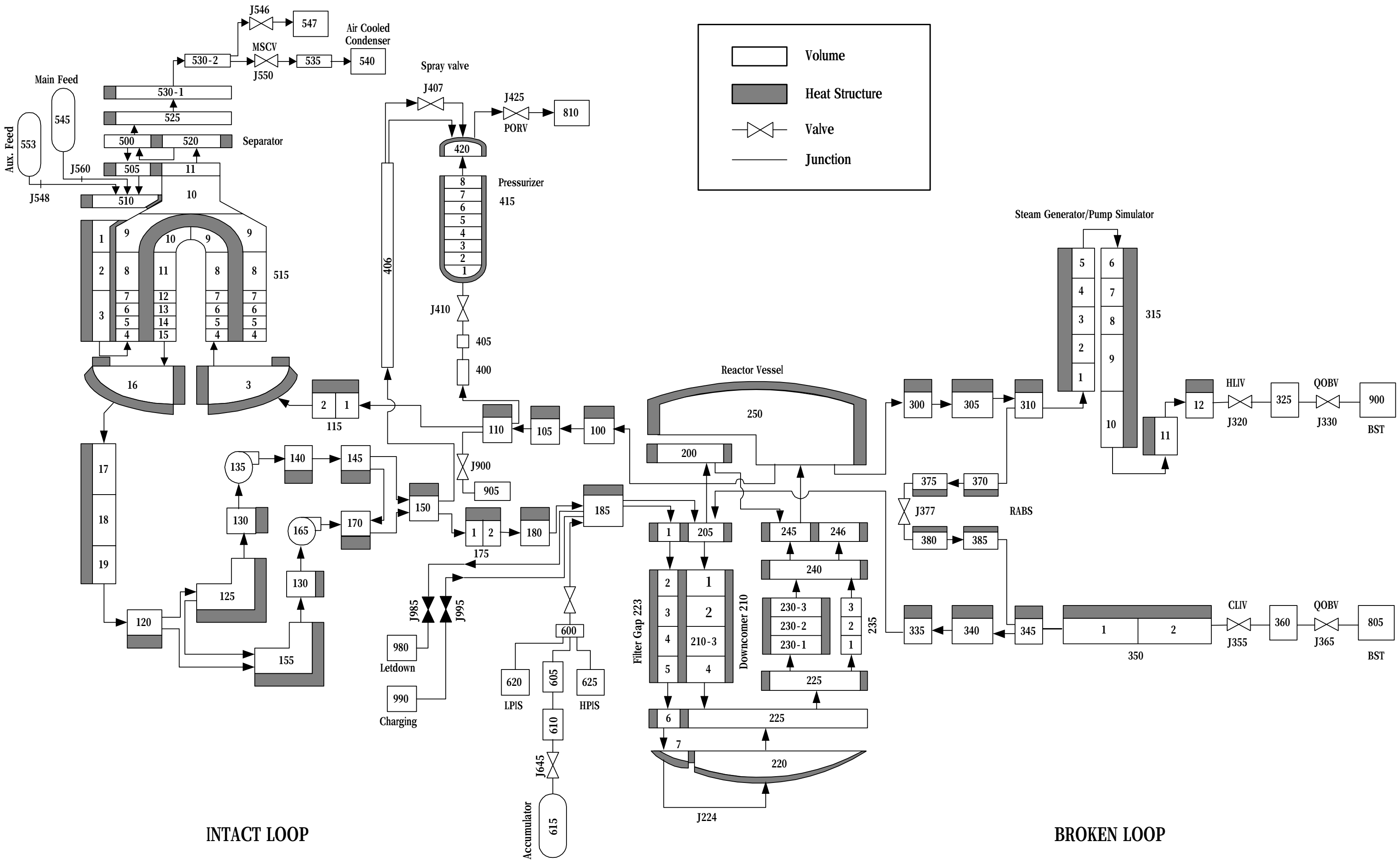

Figure 1 RELAP5 Nodalization for LOFT Test L9-1

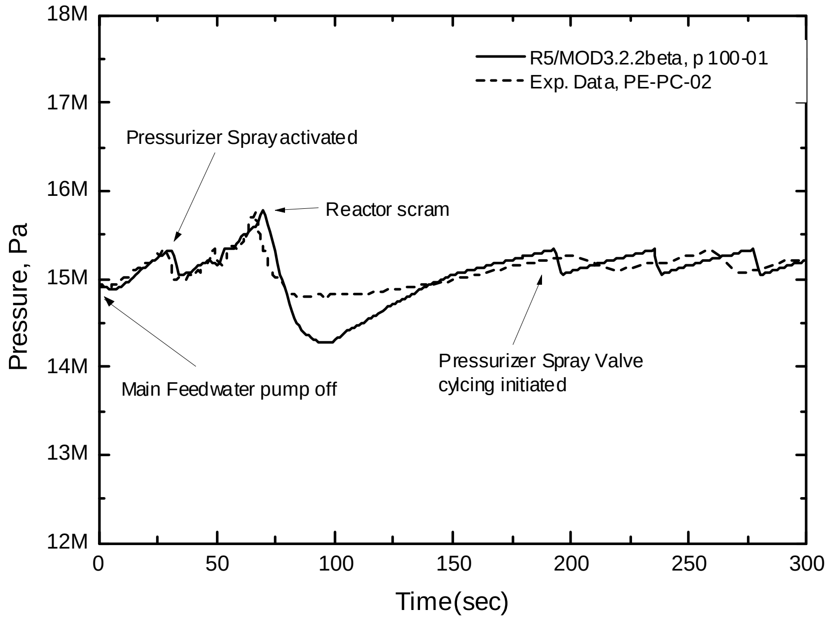

Figure 2 Comparison of pressure at the intact hot leg (short term)

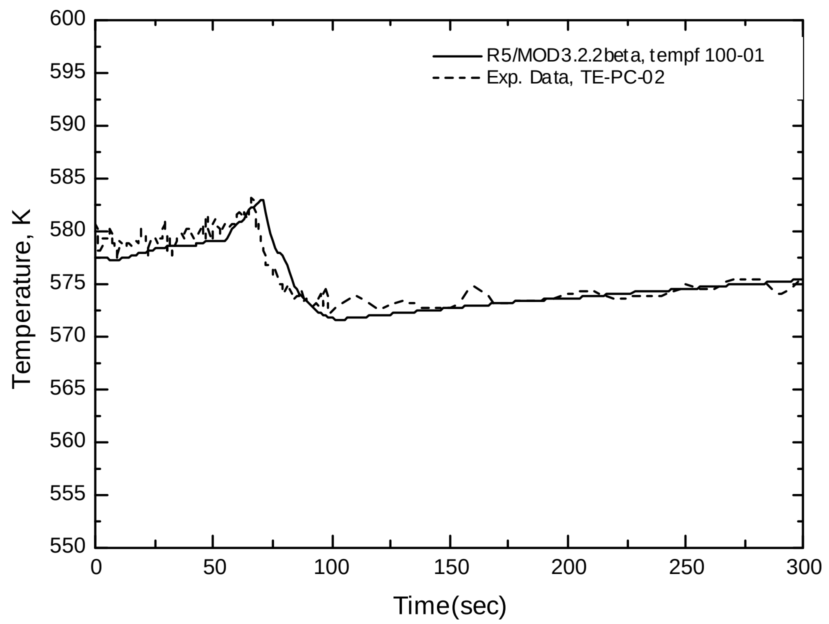

Figure 3 Comparison of temperature at the intact hot leg (short term)

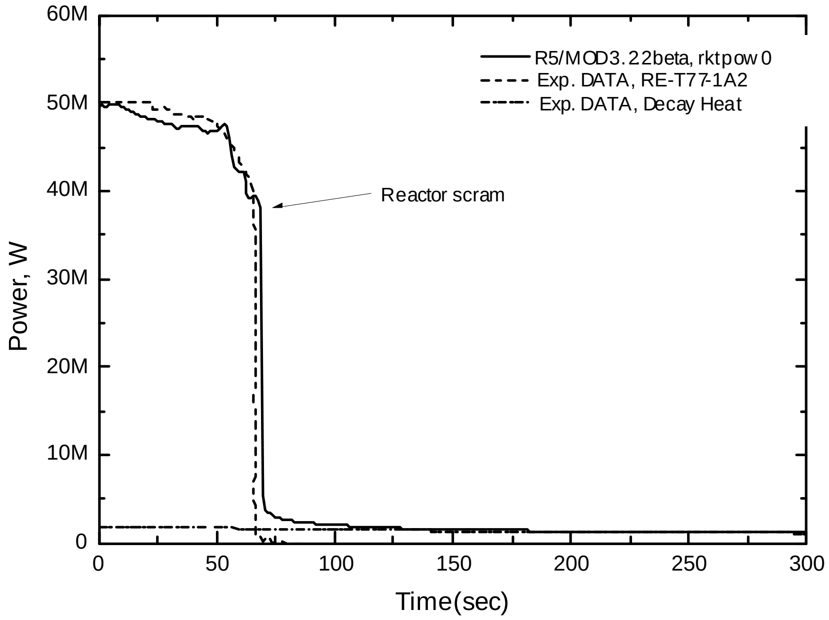

Figure 4 Comparison of reactor power

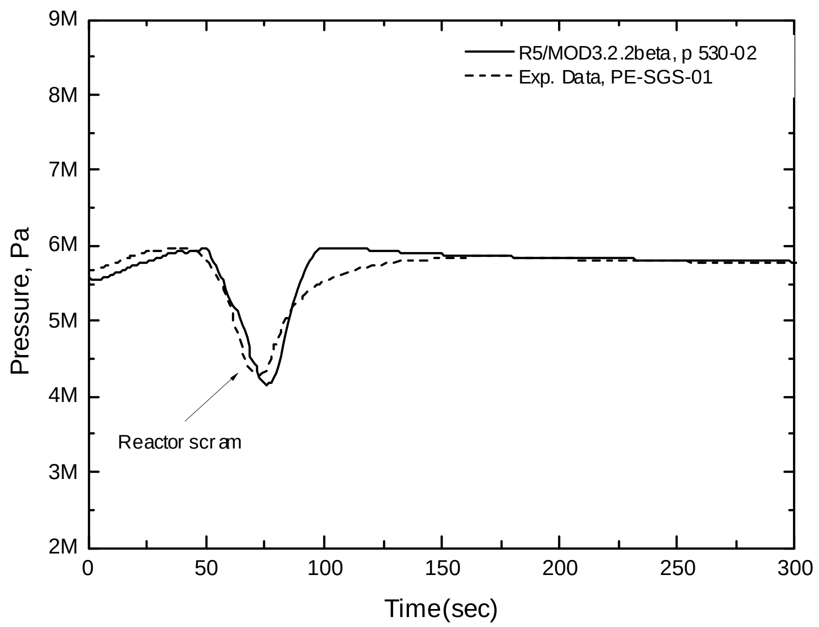

Figure 5 Comparison of pressure at the SG secondary side (short term)

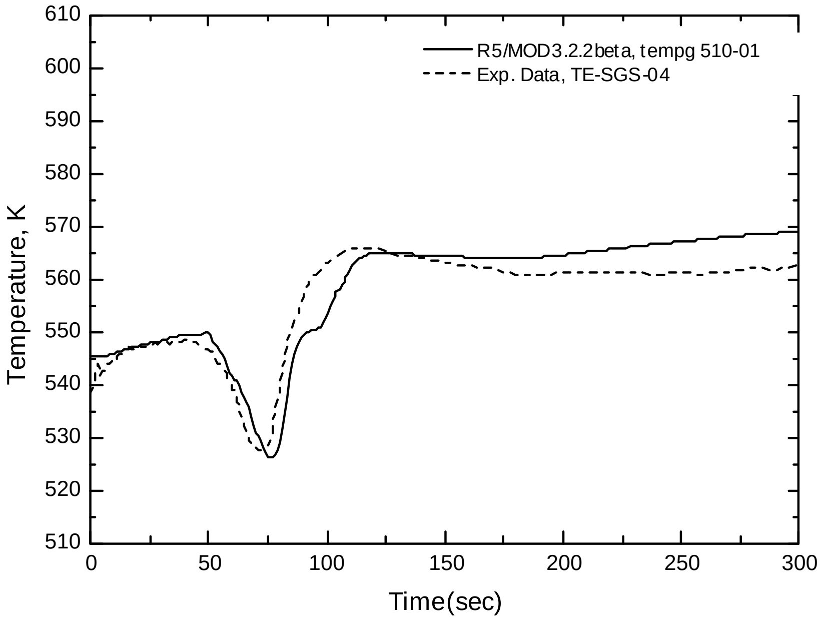

Figure 6   Comparison of temperature at the SG secondary side (short term)

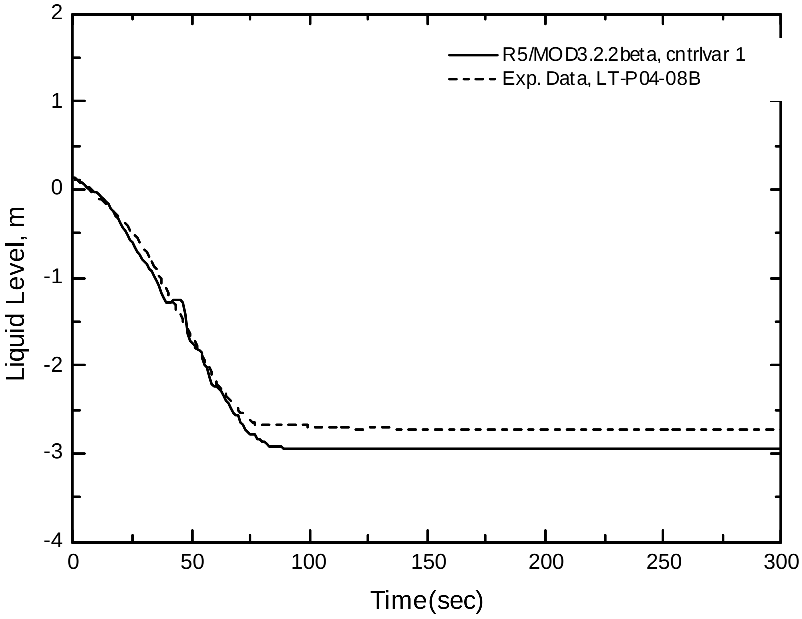

Figure 7   Comparison of SG collapsed liquid level (short term)

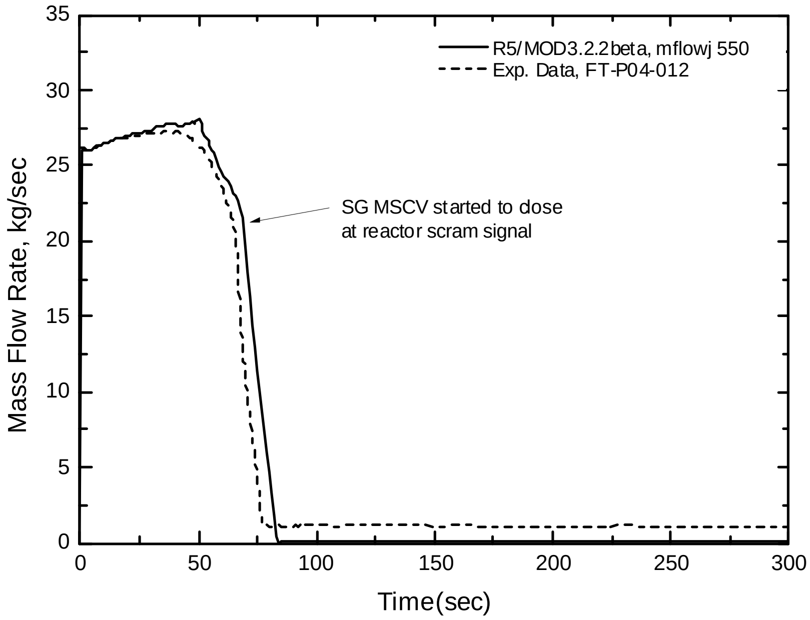

Figure 8 Comparison of mass flow rate through MSCV (short term)